



Low-loss single-mode hollow-core fiber with anisotropic anti-resonant elements

Habib, Selim; Bang, Ole; Bache, Morten

Published in:
Optics Express

Link to article, DOI:
[10.1364/OE.24.008429](https://doi.org/10.1364/OE.24.008429)

Publication date:
2016

Document Version
Publisher's PDF, also known as Version of record

[Link back to DTU Orbit](#)

Citation (APA):
Habib, S., Bang, O., & Bache, M. (2016). Low-loss single-mode hollow-core fiber with anisotropic anti-resonant elements. *Optics Express*, 24(8). <https://doi.org/10.1364/OE.24.008429>

General rights

Copyright and moral rights for the publications made accessible in the public portal are retained by the authors and/or other copyright owners and it is a condition of accessing publications that users recognise and abide by the legal requirements associated with these rights.

- Users may download and print one copy of any publication from the public portal for the purpose of private study or research.
- You may not further distribute the material or use it for any profit-making activity or commercial gain
- You may freely distribute the URL identifying the publication in the public portal

If you believe that this document breaches copyright please contact us providing details, and we will remove access to the work immediately and investigate your claim.

Low-loss single-mode hollow-core fiber with anisotropic anti-resonant elements

Md. Selim Habib,* Ole Bang, and Morten Bache

DTU Fotonik, Department of Photonics Engineering, Technical University of Denmark, DK-2800, Kgs. Lyngby, Denmark

*seha@fotonik.dtu.dk

Abstract: A hollow-core fiber using anisotropic anti-resonant tubes in the cladding is proposed for low loss and effectively single-mode guidance. We show that the loss performance and higher-order mode suppression is significantly improved by using symmetrically distributed anisotropic anti-resonant tubes in the cladding, elongated in the radial direction, when compared to using isotropic, i.e. circular, anti-resonant tubes. The effective single-mode guidance of the proposed fiber is achieved by enhancing the coupling between the cladding modes and higher-order-core modes by suitably engineering the anisotropic anti-resonant elements. With a silica-based fiber design aimed at 1.06 μm , we show that the loss extinction ratio between the higher-order core modes and the fundamental core mode can be more than 1000 in the range 1.0–1.65 μm , while the leakage loss of the fundamental core mode is below 15 dB/km in the same range.

©2016 Optical Society of America

OCIS codes: (060.4005) Microstructured fibers; (060.2310) Fiber optics; (060.2400) Fiber properties; (060.2280) Fiber design and fabrication.

References and links

1. J. C. Knight, J. Broeng, T. A. Birks, and P. S. J. Russell, "Photonic band gap guidance in optical fibers," *Science* **282**(5393), 1476–1478 (1998).
2. R. F. Cregan, B. J. Mangan, J. C. Knight, T. A. Birks, P. S. Russell, P. J. Roberts, and D. C. Allan, "Single-mode photonic band gap guidance of light in air," *Science* **285**(5433), 1537–1539 (1999).
3. P. S. J. Russell, P. Hölzer, W. Chang, A. Abdolvand, and J. C. Travers, "Hollow-core photonic crystal fibres for gas-based nonlinear optics," *Nat. Photonics* **8**(4), 278–286 (2014).
4. G. Humbert, J. Knight, G. Bouwmans, P. Russell, D. Williams, P. Roberts, and B. Mangan, "Hollow core photonic crystal fibers for beam delivery," *Opt. Express* **12**(8), 1477–1484 (2004).
5. F. Gèrôme, P. Dupriez, J. Clowes, J. C. Knight, and W. J. Wadsworth, "High power tunable femtosecond soliton source using hollow-core photonic bandgap fiber, and its use for frequency doubling," *Opt. Express* **16**(4), 2381–2386 (2008).
6. F. Gèrôme, K. Cook, A. K. George, W. J. Wadsworth, and J. C. Knight, "Delivery of sub-100fs pulses through 8m of hollow-core fiber using soliton compression," *Opt. Express* **15**(12), 7126–7131 (2007).
7. A. Urich, R. R. J. Maier, F. Yu, J. C. Knight, D. P. Hand, and J. D. Shephard, "Flexible delivery of Er:YAG radiation at 2.94 μm with negative curvature silica glass fibers: a new solution for minimally invasive surgical procedures," *Biomed. Opt. Express* **4**(2), 193–205 (2013).
8. F. Poletti, N. V. Wheeler, M. N. Petrovich, N. Baddela, E. N. Fokoua, J. R. Hayes, D. R. Gray, and D. J. Richardson, "Towards high-capacity fibre-optic communications at the speed of light in vacuum," *Nat. Photonics* **7**(4), 279–284 (2013).
9. H. Bao, K. Nielsen, H. K. Rasmussen, P. U. Jepsen, and O. Bang, "Fabrication and characterization of porous-core honeycomb bandgap THz fibers," *Opt. Express* **20**(28), 29507–29517 (2012).
10. F. Benabid and P. J. Roberts, "Linear and nonlinear optical properties of hollow core photonic crystal fiber," *J. Mod. Opt.* **58**(2), 87–124 (2011).
11. F. Yu, W. J. Wadsworth, and J. C. Knight, "Low loss silica hollow core fibers for 3–4 μm spectral region," *Opt. Express* **20**(10), 11153–11158 (2012).
12. A. F. Kosolapov, A. D. Pryamikov, A. S. Biriukov, V. S. Shiryayev, M. S. Astapovich, G. E. Snopatin, V. G. Plotnichenko, M. F. Churbanov, and E. M. Dianov, "Demonstration of CO₂-laser power delivery through chalcogenide-glass fiber with negative-curvature hollow core," *Opt. Express* **19**(25), 25723–25728 (2011).
13. W. Belardi and J. C. Knight, "Effect of core boundary curvature on the confinement losses of hollow antiresonant fibers," *Opt. Express* **21**(19), 21912–21917 (2013).

14. W. Belardi and J. C. Knight, "Hollow antiresonant fibers with reduced attenuation," *Opt. Lett.* **39**(7), 1853–1856 (2014).
15. W. Belardi and J. C. Knight, "Hollow antiresonant fibers with low bending loss," *Opt. Express* **22**(8), 10091–10096 (2014).
16. F. Poletti, "Nested antiresonant nodeless hollow core fiber," *Opt. Express* **22**(20), 23807–23828 (2014).
17. M. S. Habib, O. Bang, and M. Bache, "Low-loss hollow-core silica fibers with adjacent nested anti-resonant tubes," *Opt. Express* **23**(13), 17394–17406 (2015).
18. F. Couny, F. Benabid, P. J. Roberts, P. S. Light, and M. G. Raymer, "Generation and photonic guidance of multi-octave optical-frequency combs," *Science* **318**(5853), 1118–1121 (2007).
19. S. Février, B. Beaudou, and P. Viale, "Understanding origin of loss in large pitch hollow-core photonic crystal fibers and their design simplification," *Opt. Express* **18**(5), 5142–5150 (2010).
20. A. Argyros and J. Pla, "Hollow-core polymer fibres with a kagome lattice: potential for transmission in the infrared," *Opt. Express* **15**(12), 7713–7719 (2007).
21. B. Debord, M. Alharbi, T. Bradley, C. Fourcade-Dutin, Y. Y. Wang, L. Vincetti, F. Gérôme, and F. Benabid, "Hypocycloid-shaped hollow-core photonic crystal fiber Part I: Arc curvature effect on confinement loss," *Opt. Express* **21**(23), 28597–28608 (2013).
22. A. N. Kolyadin, A. F. Kosolapov, A. D. Pryamikov, A. S. Biriukov, V. G. Plotnichenko, and E. M. Dianov, "Light transmission in negative curvature hollow core fiber in extremely high material loss region," *Opt. Express* **21**(8), 9514–9519 (2013).
23. M. S. Habib, O. Bang, and M. Bache, "Low-loss Hollow-core Anti-Resonant Fibers with Semi-Circular Nested Tubes," *IEEE J. Sel. Top. Quantum Electron.* **22**, 4402107 (2016).
24. R. Guobin, W. Zhi, L. Shuqin, and J. Shuisheng, "Mode classification and degeneracy in photonic crystal fibers," *Opt. Express* **11**(11), 1310–1321 (2003).
25. M. C. Günendi, P. Uebel, M. H. Frosz, and P. S. J. Russell, "Broad-band robustly single-mode hollow-core PCF by resonant filtering of higher order modes," *arXiv* **1448**, 1508.06747 (2015).
26. A. Hartung, J. Kobelke, A. Schwuchow, J. Bierlich, J. Popp, M. A. Schmidt, and T. Frosch, "Low-loss single-mode guidance in large-core antiresonant hollow-core fibers," *Opt. Lett.* **40**(14), 3432–3435 (2015).
27. M. Michieletto, J. K. Lyngsø, C. Jakobsen, O. Bang, and T. T. Alkeskjold, "Hollow-core fibres for high power pulse delivery," *Opt. Express* **24**(7), 7103–7119 (2016).

1. Introduction

Light guidance in hollow-core fibers (HCFs) [1,2] has enabled new applications due to their extraordinary properties compared to solid-core fibers: when light propagates in a gas-filled core instead of glass, it propagates faster and often with low dispersion, and the gas tolerates extremely large pulse energies and allow tunable control over dispersion and nonlinearity through pressure [3]. Applications include high-power [4] and ultra-short pulse delivery [5], pulse compression [6], mid-IR transmission [7], telecommunication [8] and terahertz applications [9]. The hollow-core photonic band gap (HC-PBG) fiber is a common HCF, which guides light in the air-core using a 2D periodic cladding structure showing a photonic band gap [1]. Thus, the cladding does not support modes for a certain range of optical frequencies and propagation constants. In these ranges the core mode is not able to couple with cladding modes and is thus guided in the hollow air-core. However, the HC-PBG fiber suffers from limited transmission bandwidth [10], strong power overlap of the core modes with the glass cladding and high group-velocity dispersion (especially at the band-gap edges).

Negative-curvature HCFs are interesting alternatives, promising a low power fraction in the cladding, low dispersion, and broadband transmission [11–17]. The term "negative curvature" indicates that the surface normal to the core boundary is oppositely directed from the core [12]. The hollow-core anti-resonant (HC-AR) fiber is particularly simple as it only needs a single layer of cladding tubes. The key property of the HC-AR fiber is that it has a sequence of narrow-bandwidth high-loss regions, where the core modes become resonant (phase matched) with the cladding modes. In between these high-loss regions the core modes are anti-resonant with the cladding modes, which allow air-core confinement, i.e. low-loss transmission. The absolute amount of loss of the core modes will then depend on inhibited coupling between the core and cladding modes due to a low density of cladding modes [18–21], which is a property that can be controlled by suitable fiber design engineering. Loss is further reduced in a "node-free" design [16], where the cladding tubes do not touch each other so the core mode no longer couples to the glass cladding mode in the nodal intersections. The current challenges of HC-AR fibers are realizing loss-values comparable to HC-PBG fibers as

well as single-mode operation, achieved by increasing the loss of higher-order modes (HOMs).

HC-AR fibers with both circular AR tubes [12,15,22] as well as more intricately shaped AR tubes [11,13] have been investigated. A significant loss reduction is possible with nested tubes inside the AR tubes [14,16,17,23], but this substantially increases complexity. Here we propose a simpler solution using anisotropic AR tubes, elongated along the fiber radial direction, which allows simultaneously achieving (a) an increased negative curvature in the core, (b) a node-free design, and (c) a larger distance from the core to the outer capillary. All these properties could not be achieved simultaneously in the previous cases [11–17,22]. Importantly, these properties offer a degree of freedom in the design to reduce the losses significantly, achieve low-loss broadband transmission, and effectively suppress HOMs. Numerical results for a silica-based design targeting $1.06\ \mu\text{m}$ show that the leakage loss can be reduced 1-2 orders of magnitude (4 dB/km at $1.06\ \mu\text{m}$) compared to the standard HC-AR fiber with circular AR tubes. Moreover, the fiber is made effectively single-moded by suppressing HOMs resulting in an extinction loss ratio between the core HOMs and fundamental mode (FM) that is over 1000 in the $1.0\text{--}1.65\ \mu\text{m}$ spectral range, while the FM in the same range experiences loss $<15\ \text{dB/km}$. Such specs cannot be reproduced with the standard isotropic design without using complex designs with multiple nested AR tubes [17].

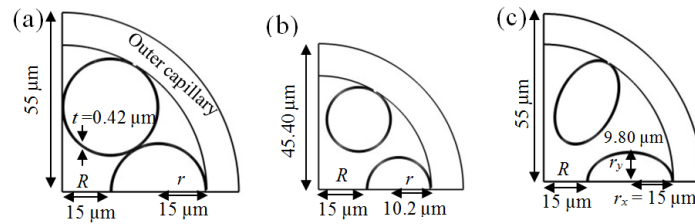


Fig. 1. Geometry of the considered HC-AR fibers, keeping fixed the core radius $R = 15\ \mu\text{m}$ and silica strut thickness $t = 0.42\ \mu\text{m}$. The structural parameters shown in the figure are those that optimized the leakage loss at $1.06\ \mu\text{m}$. The figures are scaled to indicate their relative size.

2. Numerical results

Figure 1(a)–1(c) shows the considered HC-AR fiber geometries, using a thick outer capillary with AR tubes on the inner wall. Design (a) is the usual case with touching isotropic (circular) AR cladding tubes. Starting from (a), the design is optimized for minimal losses, resulting in the circular design (b) and elliptical design (c). The latter is the proposed anisotropic AR tube design, here an ellipse squeezed in the azimuthal direction. Other anisotropic shapes are possible. We focus on a silica fiber designed for $\lambda = 1.06\ \mu\text{m}$ (i.e. for high-power Yb lasers), which has 6 AR tubes (a larger number is also feasible, and below we will specifically compare 6 vs. 8 AR tubes), a fixed core radius $R = 15\ \mu\text{m}$ (large enough to enable high-power transmission) and silica strut thickness $t = 0.42\ \mu\text{m}$ (making the first high-loss resonance occur at around $\lambda = 0.88\ \mu\text{m}$ [16]). This choice of strut thickness implies that light at $1.06\ \mu\text{m}$ is guided in the fundamental AR transmission band, which compared to the next higher-order AR transmission bands is favorable since it performs better in terms of loss and transmission bandwidth. The ellipticity is defined as $\eta = r_y/r_x$, where r_y is the radius in the azimuthal direction and r_x is the radius in the radial direction; in the following we keep $r_x = 15\ \mu\text{m}$ fixed, and $\eta < 1$ will reduce the loss. We used a quarter of the geometry for the numerical calculations because of mode symmetry [24], except for the bend loss calculations where a half geometry was used due to a reduced symmetry in the elliptical case. We used the same numerical method as explained in [17], which briefly explained relies on finite-element simulations to calculate the fiber modes and their propagation constants.

2.1 Optimization the leakage loss of the HC-ARFs

First the HC-AR fibers were optimized to get the lowest loss at $1.06\ \mu\text{m}$ by adjusting the size of the AR elements with the core size fixed (see [17] for details on the calculations). Figure 2(a) shows the leakage loss (or confinement loss, α_c) as a function of AR air-hole radius for the circular case. When the AR tube radius decreases from $r = 15$ to $10.2\ \mu\text{m}$, the leakage loss decreases to a minimum value of $30\ \text{dB/km}$, i.e. improved with around one order of magnitude. Interestingly, the AR tubes are here much smaller than the “non-touching” node-free design (i.e. where the AR tubes are reduced just enough to prevent them from touching each other), which otherwise has been considered optimal [16,22]: the reasoning has been that the core FM no longer has coupling loss to the cladding modes that in the touching-case reside in the glass intersections in these nodes. However, this would imply a sharp drop in loss as r is taken below $15\ \mu\text{m}$ to the non-touching value. Instead it is continuous, indicating that the coupling loss to the cladding modes in the glass nodes is not dominating for the chosen fiber design (however, this does not mean that for other designs it is not important), and the loss instead drops smoothly because the FM phase-mismatch to the cladding modes increases gradually. This is eventually balanced with the increased loss of the FM as its evanescent tail overlaps more with the outer capillary wall as the circles shrink. This is because we here fix the core size, so the shrinking circles imply that the outer capillary becomes closer to the core.

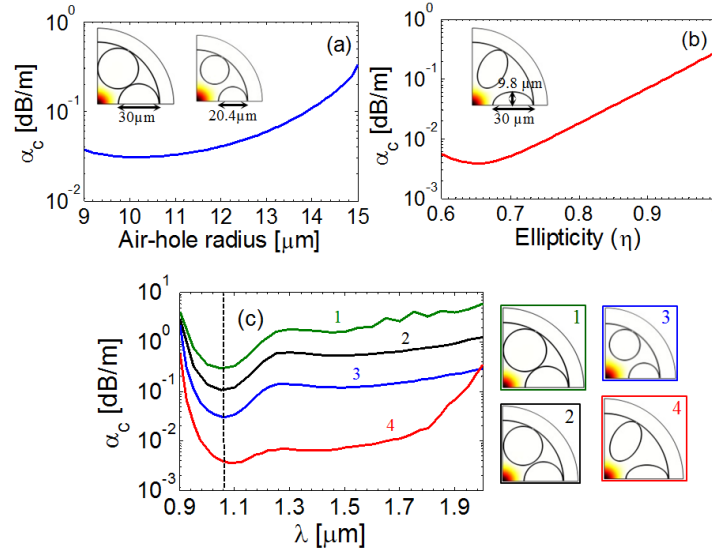


Fig. 2. Calculated leakage loss at $1.06\ \mu\text{m}$ as a function of (a) air-hole radius for circular AR tubes and (b) ellipticity of the AR tubes keeping $r_x = 15\ \mu\text{m}$. Inset: FM field profiles at $1.06\ \mu\text{m}$. (c) Loss vs. wavelength for different HC-AR fibers (dashed line: $\lambda = 1.06\ \mu\text{m}$). All structures have the same core radius $R = 15\ \mu\text{m}$ and uniform silica strut thickness $t = 0.42\ \mu\text{m}$.

Figure 2(b) shows the leakage loss for the elliptical case. As we fix the core size and decrease η , the major axis (in radial direction) is fixed at $r_x = 15\ \mu\text{m}$, and the minor axis (in the azimuthal direction) changes from $r_y = 15$ to $9\ \mu\text{m}$. The lowest leakage loss of $4\ \text{dB/km}$ was obtained for $\eta = 0.65$, i.e., $r_x = 15\ \mu\text{m}$ and $r_y = 9.80\ \mu\text{m}$. Thus, orders of magnitude improvement is realized by squeezing the azimuthal axis of the AR tubes. The minimum has a different explanation than the circular case, because we are here able to fix the distance from the core to the outer capillary. Instead the loss improvement obtained for $\eta < 1$ is due to an increased phase mismatch between the FM and cladding modes is eventually balanced by an increased leakage loss as the FM starts leaking into the voids between the ever slimmer AR ellipses.

Figure 2(c) depicts the spectral loss distribution for different HC-AR fibers. Curves 1-3 show the circular cases: case 1 (green) where the tube walls are touching each other, thus forming glass nodes in the cladding, and case 2 when the air-hole radius is reduced to $14\ \mu\text{m}$ so the AR tubes no longer touch each other (black). Case 3 (blue) shows the additional reduction of leakage loss until the minimum is reached, achieved as mentioned above by shrinking the circular tubes further (thus separating them further). Finally, case 4 (red) shows the elliptical design, displaying significantly improved loss performance; the leakage loss is over one order of magnitude lower than for the best circular design. Moreover, the low-loss range spans nearly the entire near-IR, which is promising for broadband ultrafast applications.

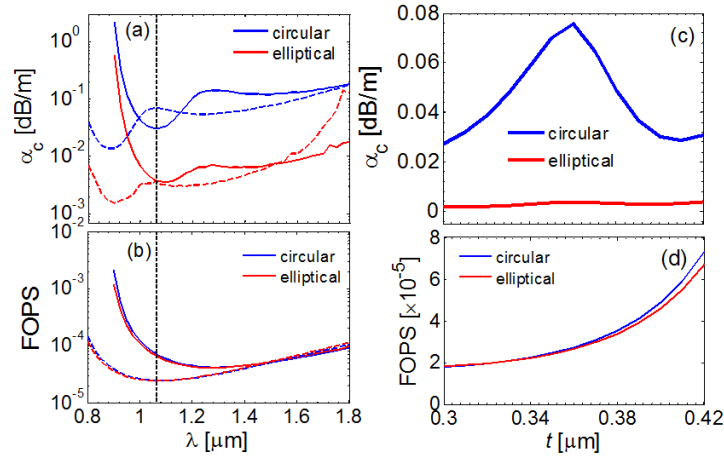


Fig. 3. Calculated (a) leakage loss and (b) fraction of power in silica (FOPS) vs. wavelength for different strut thicknesses. Solid lines and dashed lines are calculated for $t = 0.42\ \mu\text{m}$ and $t = 0.35\ \mu\text{m}$ respectively; (c) Leakage loss and (d) FOPS vs. strut thickness at $1.06\ \mu\text{m}$.

2.2 Scaling the strut thickness

One of the limiting factors in high-power beam delivery is the so-called fraction of power in silica (FOPS), i.e., the optical power overlap with the silica cladding, which should be kept small. Figure 3(b) shows that FOPS can be reduced by reducing the strut thickness of silica ($\sim 2 \times 10^{-5}$ at $1.06\ \mu\text{m}$ for $t = 0.35\ \mu\text{m}$), which is several orders of magnitude lower than the HC-PBG [4]. This makes HC-AR fibers an ideal medium to explore propagation of high power beam delivery. When comparing FOPS for circles and ellipses the performance is similar, but the advantage in using ellipses comes in terms of leakage loss, see Fig. 3(a), which has a local minimum at a wavelength controlled by the strut thickness. As the strut thickness is reduced, this minimum shifts towards lower wavelengths, but at the wavelength of $1.06\ \mu\text{m}$ that the design is intended for the leakage loss becomes quite high as the strut thickness is reduced. In the elliptical case the wavelength loss-variation is instead much more flat, so the leakage loss at $1.06\ \mu\text{m}$ varies only little when the strut thickness is reduced. Figure 3(c)-3(d) summarizes these trends by showing the leakage loss and FOPS vs. strut thickness at $1.06\ \mu\text{m}$ for both cases: elliptical tubes have one order of magnitude lower losses compared to circular tubes when the strut thickness varies from 0.35 to $0.42\ \mu\text{m}$ (note the y-axis is linear); in turn the FOPS is almost the same for both cases. The elliptical design will therefore allow for more design degrees of freedom. Note that $t = 0.35\ \mu\text{m}$ is generally considered a practical limit for proper fiber cleaving, rather than a fabrication limit. This limit is less severe for silica HC-AR fibers at longer wavelengths as this demands larger strut thicknesses, in which case the potential of the elliptical design can be exploited fully.

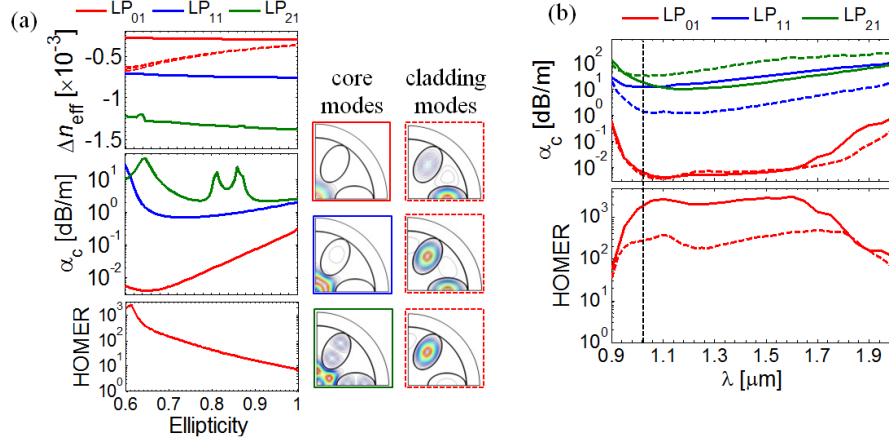


Fig. 4. (a) Relative effective index, loss and HOMER vs. ellipticity for $\lambda = 1.06 \mu\text{m}$. (b) Spectral loss and HOMER curves (full lines: $\eta = 0.61$, dashed lines: $\eta = 0.65$). $t = 0.42 \mu\text{m}$ was used.

2.3 Effectively single-mode operation

HC-AR fibers with large cores are not single-moded, but they can be made effectively single-moded by engineering the shape and size of the AR tubes so the HOMs experience more loss than the FM [17]. Figure 4(a) shows the relative effective indices ($\Delta n_{\text{eff}} = n_{\text{eff}} - 1$) of the first three core modes (here denoted LP₀₁, LP₁₁, and LP₂₁) and the first three cladding modes. The core FM (LP₀₁) has the highest Δn_{eff} , which remains constant as a function of ellipticity. The first three cladding modes have only slightly larger Δn_{eff} than the first core HOM (LP₁₁) because the core area is only a few times larger than the area of a single cladding tube. Thus, the first HOM is located within the domain of the cladding modes, which increases phase matching to cladding modes [25,26]. This effect is more evident for the strongly elliptical AR tubes ($\eta \sim 0.60$ - 0.70), where the cladding modes are better phase-matched to the HOMs than to the FM, which effectively suppresses the guidance of the HOMs due to higher losses.

The FM loss decreases much more than the HOM loss when the ellipticity is decreased, and in the $\eta = 0.60$ - 0.70 range the HOM losses even start increasing while the FM loss remains at 4 dB/km. This shows how the HOM losses can be made higher by suitably choosing the ellipticity. The aim is maximizing the so-called HOM extinction ratio (HOMER), defined as the ratio between the loss of the HOM with the lowest loss and the FM loss [16]. The maximum HOMER was found to be ~ 2500 at $\eta \sim 0.61$, while at $\eta = 0.65$, where the lowest FM loss was found at $1.06 \mu\text{m}$, a HOMER of ~ 200 is found; both high enough to make the fibers effectively single-moded. Remarkably, the $\eta = 0.61$ case is only slightly more lossy (5 dB/km) than the $\eta = 0.65$ case, so the loss penalty of maximizing HOMER is small. This again shows the design freedom of the anisotropic AR elements. The spectral loss and HOMER is shown in Fig. 4(b). The HOMER for the design with the lowest loss at $1.06 \mu\text{m}$ ($\eta = 0.65$) can be made in excess of 150 between $\lambda = 0.95$ - $1.8 \mu\text{m}$, while keeping $\alpha_c < 15$ dB/km. Thus, this fiber has low-loss and is effectively single-moded over an octave of bandwidth. Interestingly, when the loss is increased slightly to maximize HOMER ($\eta = 0.61$), $\text{HOMER} > 1000$ between $\lambda = 1.0$ - $1.75 \mu\text{m}$ with $\alpha_c < 15$ dB/km from $\lambda = 1.0$ - $1.65 \mu\text{m}$. Figure 5(a) shows HOMER vs. wavelength, and confirms that the elliptical case outperforms the circular case in the entire wavelength regime 0.9 - $2 \mu\text{m}$. Figure 5(b) shows the bend loss (α_b) of the considered structures, calculated in both the x and y directions. The elliptical case shows an azimuthal variation of the bend loss, evidenced by a loss peak seen only in the x -direction for low bending radii due to increased core-cladding mode coupling. Therefore the

circular case shows better bend loss performance for low bend radii for the 6-tube structure studied here.

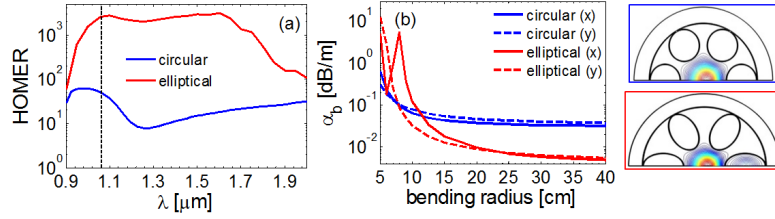


Fig. 5. (a) Wavelength dependence of HOMER for circular ($r = 10.2\mu\text{m}$) and elliptical ($\eta = 0.61$) AR tubes (b) Bend loss vs bend radius for circular ($r = 10.2\mu\text{m}$) and elliptical ($\eta = 0.65$) AR tubes with $t = 0.42 \mu\text{m}$. The FM profiles are shown in the right hand side for a 10 cm bending radius.

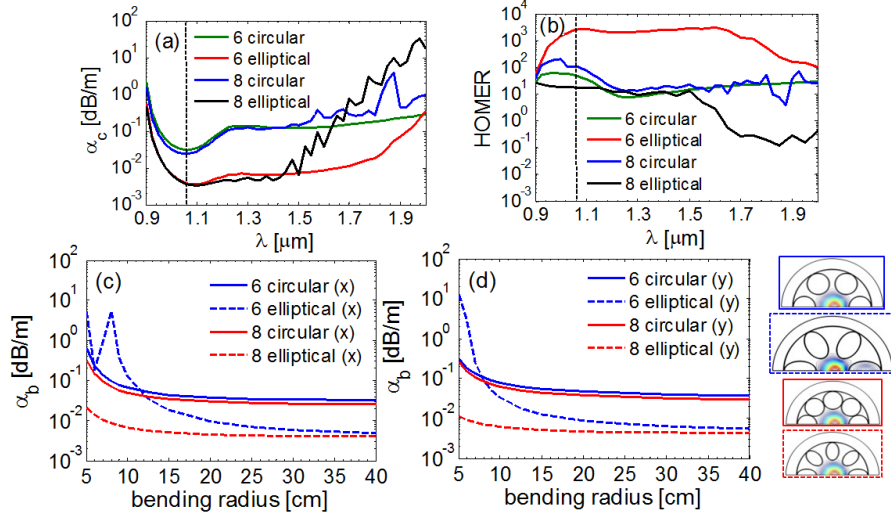


Fig. 6. (a) Loss vs. wavelength (b) HOMER (c-d) Bending loss vs. bending radius for different HC-AR fibers. All structures have same core radius $R = 15 \mu\text{m}$ and uniform silica strut thickness $t = 0.42 \mu\text{m}$. All fiber designs are optimized at $1.06 \mu\text{m}$ to give minimum leakage loss. The contour plots of the fundamental air-core mode distribution are shown in the right hand side for a 10 cm bending radius. The color of the frame corresponds to the color of the line in the plot.

2.4 Comparison with other design cases

In Fig. 6 we compare the loss performance and HOMER of 6 and 8 AR tubes. The calculated loss spectra in Fig. 6(a) shows that 6 and 8 AR tubes have similar loss performance in the 0.9-1.45 μm spectral regime; the 8 tube cases have slightly lower losses, but using 6 tubes gives much broader low-loss transmission window for both circular and elliptical cases. We also note that the 6 tube cases (both circular and elliptical) are very smooth while the 8 tube cases show spectral fluctuations vs. wavelength at the end of the transmission window. Similar fluctuations have previously been attributed to presence of nodes in the cladding [16], but clearly the origin here is different as there are no nodes. The reason is instead found in the fact that for 8 tubes the core mode for longer wavelengths expands its mode field diameter so that it starts interacting weakly with cladding modes found at the outer capillary wall [27]; this leads to the observed fluctuations. Figure 6(b) shows the HOMER from which we see that 6 elliptical AR tubes have much higher HOMER compared to 8 AR tubes in the whole spectral regime. Finally, Figs. 6 (c)-6(d) show the bend loss performance in the x - and y - directions, respectively. For 8 AR tubes the elliptical case has better bend loss performance than the

circular case. We believe this is because for the 8 tubes case, the AR tubes are smaller compared to the 6 tubes case. Therefore for small bend radius, 6 AR tubes have coupling between the core modes and tube modes due to the larger AR tubes whereas the coupling is reduced in 8 AR tubes because of the smaller AR tubes. Figure 6 also shows contour plots of the fundamental modes for 10 cm bending radius in which for 6 AR tubes there is a coupling between the core modes and tube modes whereas for 8 AR tubes there is no coupling between the core modes and tube modes. Therefore, choosing 6 or 8 tubes would have to be a compromise in terms of whether loss bandwidth, HOMER or bend loss is the most important feature.

We also considered introducing the ellipticity from the optimized circular design (10.2 μm AR tube radius), but instead of squeezing the ellipse azimuthally, it was elongated radially (i.e. extending the major axis) while keeping the core size fixed. This implies that the outer capillary expands its size as the ellipticity drops, which results in an improved loss performance compared to shrinking the minor axis (the case we have discussed so far). However, our calculations showed that the HOMER could not reach the same high values as found in Fig. 5(a). This implies that it is harder to reduce the phase-mismatch between the core HOMs and the cladding modes when extending the major axis.

3. Conclusion

In summary, a novel hollow-core anti-resonant fiber design has been proposed, in which the anti-resonant elements in the cladding are anisotropic in shape, in contrast to the conventional isotropic circular shape. Numerical simulations using an elliptical shape as the anisotropic cladding element showed loss performances and effective single-mode guidance that could not be achieved with isotropic (circular) cladding elements. In both cases the guiding of light in the core is based on the anti-resonances of the struts in the cladding and the inhibited coupling mechanism. However, the anisotropic shape has improved performance because it simultaneously offers: (a) strong negative curvature in the core, (b) node-free (non-touching) anti-resonant elements, and (c) larger distance from the core to the outer capillary for a given core curvature. This gives a design degree-of-freedom essential for enhancing the performance, e.g. by fixing the size of the core and outer capillary while tuning the ellipticity to minimize loss. We studied a specific case, where a silica-based fiber was optimized for the Yb-laser wavelength of 1.06 μm . The HOM extinction ratio was over 1000 in the range $\lambda = 1.0\text{--}1.75$ μm with FM loss <5 dB/km at 1.06 μm and <15 dB/km for $\lambda = 1.0\text{--}1.65$ μm , which relied on increasing HOM loss by reducing the phase-mismatch between them and the cladding modes, while still maintaining a large phase-mismatch between the FM and the cladding modes. These properties are extremely promising for ultra-fast extreme nonlinear optics applications exploiting fiber-based light-matter interaction [3]. The proposed design is generic, irrespective of glass composition and target wavelength, and we expect it to improve almost any type of hollow-core fiber design exploiting the anti-resonant effect.